Acoustic waveform modeling and its problems

Weijun Zhao[1)], Yeonghwa Kim[1)]

[1)] Dept. of Geophysics, Kangwon National University, Korea, weijun_zhao@hotmail.com

Abstract: The acoustic array waveforms are simulated in a simple borehole model for both monopole and dipole sources. The model is based on the parameters obtained by the semblance processing of field waveforms collected on the physical models whose physical parameters are known. Both the synthetic and field waveforms are compared to understand the sonic waveform as well as the source wavelet characteristics.

Keywords: sonic, waveform, monopole, dipole, synthetic model, semblance

1. INTRODUCTION

Acoustic logging is an important method for petroleum exploration as well as for geotechnical applications. Many papers published are related to petroleum sonic logging in borehole of larger than 10 cm radius. In this study, the borehole is geotechnical smaller one of typical 3.8 cm radius. Short separation between source and receivers is a critical problem in geotechnical sonic log. The fact that we do not have exact information of source wavelet is another critical problem. In this study, a waveform simulation method was adopted for both monopole and dipole sources in simple borehole model according to the Kurjian and Chang's method (1986). Numerical computation is performed by the Discrete Wavenumber Method (Bouchon, 2003). The field acoustic data of both monopole and dipole sources are collected in KLW-3 test borehole located in Kangwon National University. The semblance method was applied to the field acoustic data. The estimated P- and S- head wave velocities were taken as the input parameters for waveform modeling, assuming other physical parameters are known. The semblance processing results are well consistent for both synthetic and actual data.

2. MODELING METHOD

The mathematical model is a simple fluid-filled borehole surrounded by infinite homogeneous elastic rock formation. Monopole and dipole sources are adopted here in cylindrical coordinate (r,θ,z) .The monopole source is considered as a point source located at the origin. The dipole source is considered as two point sources located at a horizontal circle of radius δ with opposite sign: one is located at $(\delta,0,0)$, the other is located at $(\delta,\pi,0)$. We followed the method described in Kurkjian and Chang (1986). The Discrete wavenumber method (Bouchon, 2003) is applied into the synthetic waveforms. The receivers in this study are limited on the axis of borehole.

For monopole source, the volume change function in frequency domain is given by (Chen, et. al., 1996)

$$V_0(\omega)= \frac{1}{\omega^2}\frac{8\alpha\omega_0(\alpha-i\omega)}{\left[(\alpha-i\omega)^2+\omega_0^2\right]^2}\ , \qquad (1)$$

where α is damping factor and ω_0 is center angular frequency. For dipole sources, the volume change function in frequency domain is given by (Tsang and Rader, 1979)

$$V_0(\omega)=\frac{8\alpha\omega_0(\alpha-i\omega)}{\left[(\alpha-i\omega)^2+\omega_0^2\right]^2} \quad . \tag{2}$$

3. COMPARISION OF WAVEFORMS

The acoustic probe used for the data acquisition is a variable frequency tool with monopole and dipole transmitters. There are single transmitter and three receivers for both monopole and dipole sources. The spacing between the transmitter and the first receiver is 0.9144 m (3 ft). The inter-receiver spacing is 0.3048 m (1 ft). The time sampling is 4 μs , the number of time sample is 512. The hold-off time is a input parameter that must be set in data acquisition. It is the start time of waveform record after source firing. Although the start time of waveforms is zero in subsequent figures, it is essentially hold-off time. The hold-off time is 50 μs for monopole data, while it is 150 μs for dipole data.

We have collected acoustic data for monopole and dipole sources in two runs separately in KLW-3 test borehole on campus at Kangwon National University. The borehole model is built for calibrating the gamma-gamma probe. The acoustic waveforms recorded at the calibration zone are extracted for processing. In addition, the formation densities are available through core measurement. The radius of the borehole is 3.8 cm consistently.

3.1 Monopole waveforms

The array waveforms of monopole source of 20 kHz are illustrated in Fig. 2(a). The existence of P and S head waves are clear from the observations of waveform variation. Fig. 2(b) shows the result of semblance (Kimball and Marzetta, 1984) employed for the waveforms. This shows that the semblance value is very high for the both head waves as well as Stoneley wave, which indicates that the processing results are much reliable. The P and S head velocities are 3420 and 2050 m/s, respectively. The hole fluid is assumed to be pure water having the velocity of 1.5 km/s and the density of 1.0 g/cm^3 . The formation density of calibration zone is 2.05 g/cm^3 . We do not have the exact information about source wavelet for our sonic logger, and the wavelet source was borrowed from Tsang and Rader (1979).

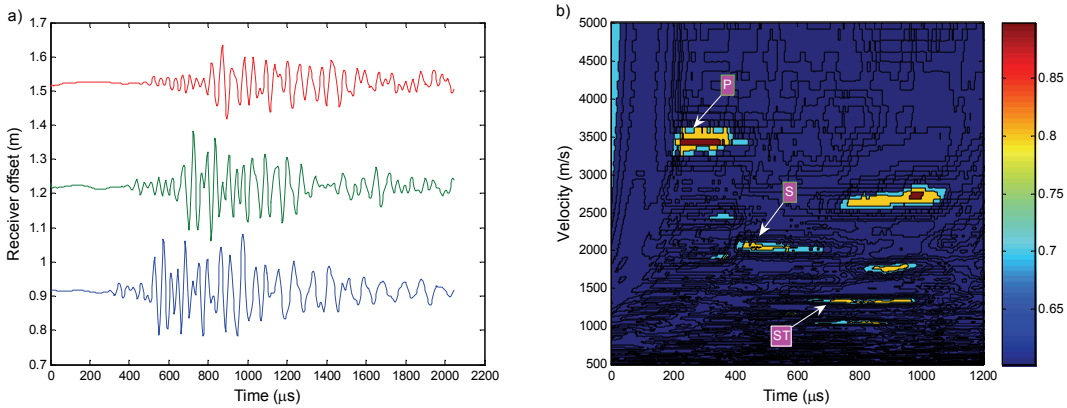

Fig. 2 Field array waveforms (a) of monopole source with center frequency of 20 kHz. The transmitter is located at 3.908 m in KLW-3 test borehole. Contour plot (b) of semblance versus arrival time and velocity for array waveforms (a). P, S and ST denote P- and S- head wave, and Stoneley wave.

Fig. 3 shows the synthetic pressure waveforms whose amplitudes are normalized by the maximum amplitude of three waveform traces. It was obtained from monopole source of 20 kHz center frequency. In Fig. 3(a), The P and S head wave arrival times on each receiver can be picked. Because P-head wave is followed by P leaky wave which is a kind of attenuative dispersive wave mode(Paillet, 1991), S-head wave is hard to be identified on field waveforms visually for monopole source. This figure shows that the first arrival of S wave is clearer with the increase of separation between source and receiver. This implies the effect of P leaky wave on the determination of first arrival of S wave. Because P leaky wave is attenuative, with the increase of offset on the z axis and the corresponding increase of P-S time, the S wave arrival becomes clearer, and it is easier to pick the first arrivals. Receiver 1 shows the worst S arrival.
The semblance result of the waveforms in Fig. 3(a) is illustrated in Fig. 3(b). The velocities of P and S head wave are 3420 and 2050 m/s, respectively. Comparison between Fig. 2(b) and Fig. 3(b) indicates that both the field and the synthetic waveforms reveal nearly the same high coherence. This supports the high coherence exists in field waveforms.

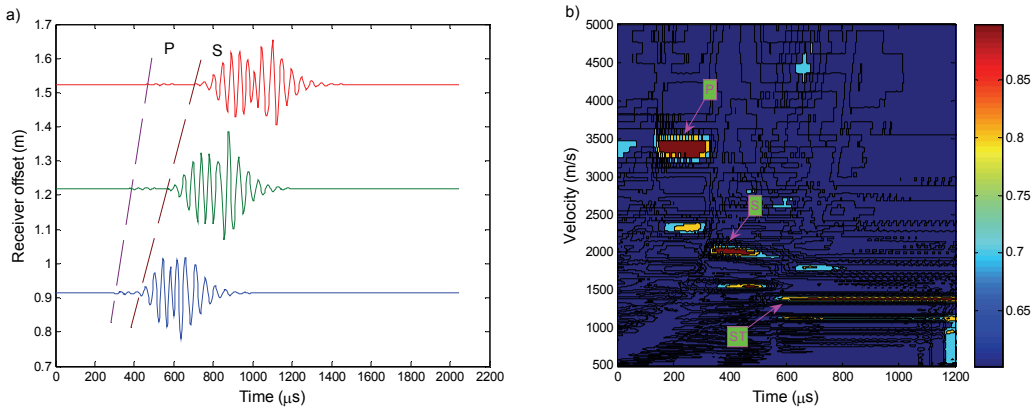

Fig.3. (a): Synthetic pressure waveforms with monopole source of 20 kHz center frequency. The two dashed lines, marked by P and S, indicate the P- and S- head wave arrivals, respectively. The arrival times of head waves are predicted by theoretical ray travel times. (b): Contour plot of semblance versus arrival time and velocity for array waveforms. The P- and S-head wave arrivals(denoted as P and S) are picked.

Fig. 4 shows the comparison of synthetic waveforms and field waveforms up to the travel time of 900 μs . Travel times of a refracted head wave should be linear with receiver offset. This seems be true for both P1 and P2 lines. The time difference between P-head wave peak in synthetic waveforms and field waveforms are about 12 μs . The line S1 denotes the trace of first trough of S- head wave on the synthetic waveforms, and S2 the first peaks on the field waveforms after the S1 arrival. Lines S1 and S2 also can be matched each other. One problem is that the waveforms around shear wave arrivals show closer coherence between receivers 2 and 3 while worse coherence between receivers 2 and 1 or 3 and 1.

3.2 Dipole waveforms

Fig. 5(a) shows the field flexural waveforms obtained from KLW-3. Fig. 6(b) gives the S- wave velocity of 2060 m/s. Although this is from dipole source, the P wave arrival is also detected with small strips showing its velocity of about 3350 m/s, slightly different from the monopole P velocity of 3420 m/s. In this study, the P velocity of 3420 m/s obtained from monopole data and the S wave velocity of 2060 m/s obtained from dipole data were used for synthetic waveforms with the water velocity of 1500 m/s, water density of 1.0 g/cm^3 , formation density of 2.05 g/cm^3 , and the borehole radius of 3.8 cm. The center frequency of source function is 5 kHz.

Hold-off time for dipole waveforms in Fig. 6 is 150 μs for each trace. For the dipole source, P head wave was observed before the S wave in field waveforms. But in semblance, a significant long strip of high semblance value implies that it is dispersive. At the onset of long strip, the S head wave can be picked visually as 2060 m/s. It is found that the theoretical arrivals coincide with the troughs of three field waveforms. In our synthetic waveforms, the amplitudes are non-zero before the S head wave arrival. Although the reason is not clear at the moment, this phenomenon also takes place on field waveforms. The difference is that the field waveforms are very weak before S wave arrivals, contrary to synthetic waveforms.

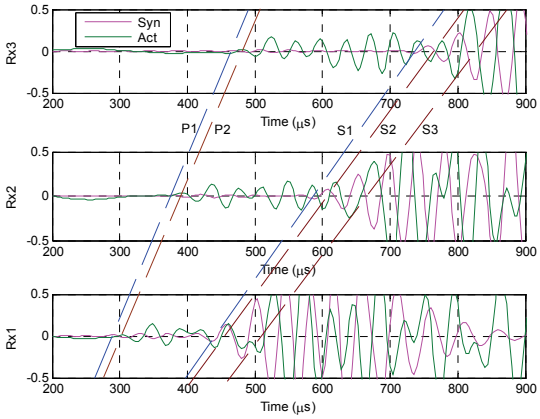

Fig. 4. Comparison of synthetic waveforms(red) and field waveforms(green). Line P1 denotes the trace of first peak of P-head wave on synthetic waveforms, while P2 denotes the trace of first peak of P-head wave on field waveforms. The line S1 denotes the trace of first trough of S-head wave on the synthetic waveforms, and S2 the first peaks on the field waveforms after the S1 arrival.

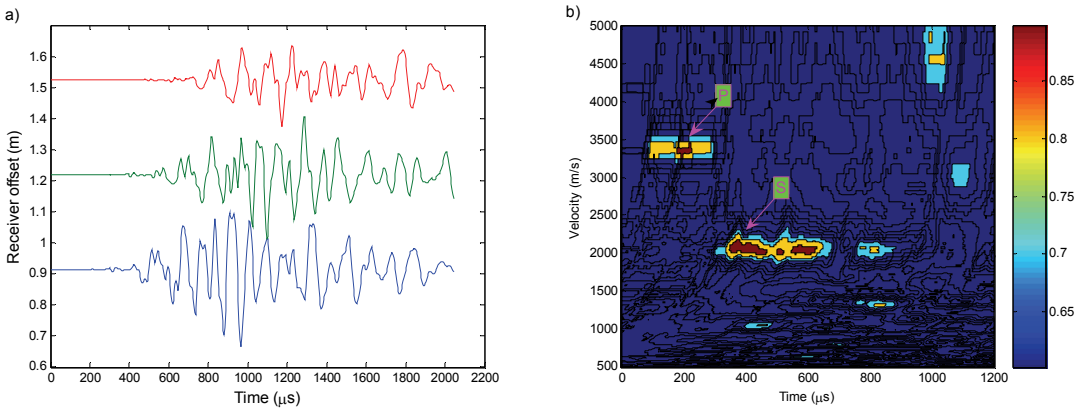

Fig.5 a) Field array waveforms of dipole sources with center frequency of 5 kHz. The transmitter is located at 3.958 m depth in KLW-3 test borehole. b) Contour plot of semblance versus arrival time and velocity for array waveforms (a).

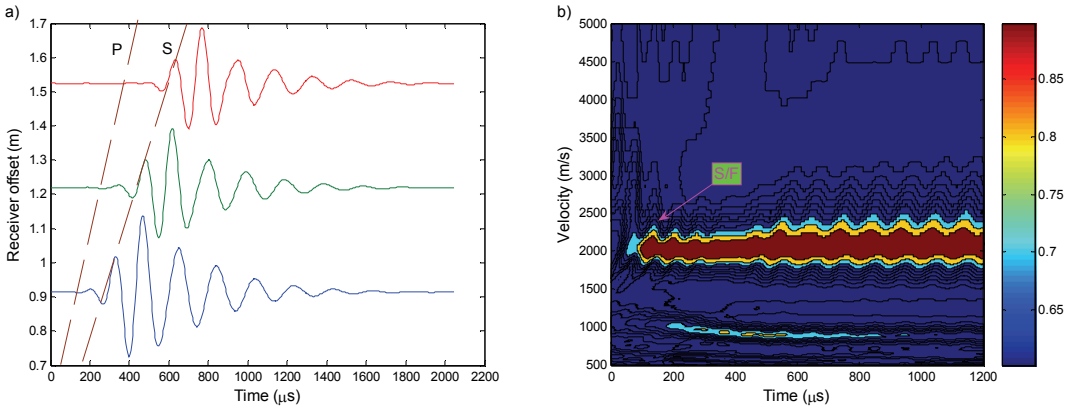

Fig.6. a) Synthetic array waveforms of dipole sources with the center frequency of 5 kHz. The waveforms are normalized by the maximum amplitude of three traces. The dashed lines denoted by P and S correspond to P and S head wave arrivals predicted by ray theory, respectively.
b) Contour plot of semblance versus arrival time and velocity for array waveforms in (a).

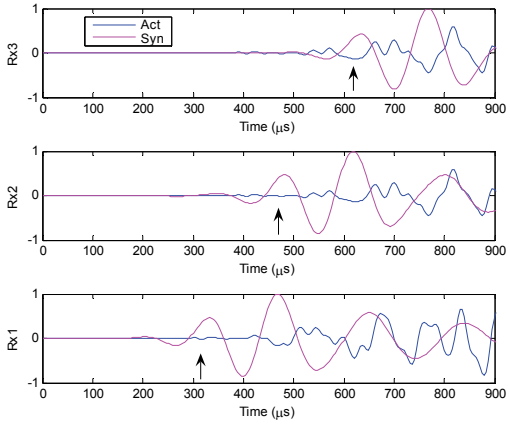

Fig. 7 Comparison of synthetic waveforms in Fig. 5 with Field waveforms in Fig. 6 on earlier part. Each trace is normalized by its maximum amplitude. The arrows mark the arrival time of S head wave predicted by ray theory.

4. CONCLUSIONS AND DISCUSSIONS

The modeling of dipole and monopole waveforms has been made in terms of P and S wave velocities obtained from semblance processing of field waveforms. Both synthetic and field waveforms are compared to understand the sonic waveform as well as the source wavelet characteristics. For monopole source, the synthetic P head wave arrivals are in agreement with the field P- head wave arrivals. The only difference is that synthetic P wave amplitude is much weaker than the field P wave. Synthetic monopole waveforms indicate that suppressing P leaky wave is very critical in picking S wave arrivals exactly. In dipole sources, most of the energy concentrate on flexural waves, although P wave arrival is also detected with small strips. It is found that the theoretical arrivals coincide with the troughs of three field waveforms. In our synthetic waveforms, the amplitudes are non-zero before the S head wave arrival. Although the reason is not clear at the moment, this phenomenon also takes place on field waveforms. The

difference is that the field waveforms are very weak before S wave arrivals, contrary to synthetic waveforms. On the other hand, the semblance processing results are much consistent for Field and synthetic waveforms of both monopole and dipole sources. Of course, comparison between the field and synthetic waveforms is not sufficient at the moment. This seems to be due to the short separation between source and receivers and/or inexact information of source wavelet. The improvement in these two problems will be expected to increase the usefulness of simulated waveforms.

5. REFERENCES

Bouchon, M., 2003, A review of the Discrete Wavenumber Method, *Pure and Applied Geophysics*, **160**, 445-465.

Chen, X. , Quan, Y., and Harris, J. M., 1996, Seimsogram synthesis for radially layered media using the generalized reflection/transmission coefficients method: Therory and applications to acoustic logging, **61**,1150-1159.

Cheng, C. H. and Toksoz, M. N., 1981, Elastic wave propagation in a fluid-filled borehole and synthetic acoustic logs, *Geophysics*, **46**, 1042-1053.

Kimball, C. V., and Marzetta, A. B., 1984, Semblance processing of borehole acoustic array data, *Geophysics*, **49**, 274-281.

Kurjian, A. L. and Chang, S. K., 1986, Acoustic multipole sources in fluid-filled boreholes, *Geophysics*, **51**, 148-163.

Paillet, F. L. and Cheng, C. H., 1991, *Acoustic waves in Boreholes,* CRC Press, Inc., 264 p.

Tsang, L. and Rader, D., 1979, Numerical evaluation of the transient acoustic waveform due to a point source in a fluid-filled borehole, *Geophysics,* **44**, 1706-1720.